

ARTICLE

Development of corrosion-stable dual-Si-layered membranes for hydrogen production via thermochemical iodine-sulfur processOdtsetseg Myagmarjav^{a*}, Nobuyuki Tanaka^a, Hiroki Noguchi^a, Yu Kamiji^a, Masato Ono^a,
Chihiro Sugimoto^a, Hajime Kon^b, Mikihiro Nomura^c and Hiroaki Takegami^a^a Department of HTTR, Japan Atomic Energy Agency, 4002 Narita-cho, Oarai, Ibaraki 311-1393, Japan;^b Energy Technology Department, Dainichi Machine and Engineering Co., Ltd., 1-11-15 Nishiku, Yokohama,
Kanagawa 220-0004, Japan;^c Department of Applied Chemistry, Shibaura Institute of Technology, 3-7-5 Toyosu, Koto-ku, Tokyo
135-8548, Japan

Hydrogen plays an important role in the transition to clean energy and the achievement of net-zero emissions. Thermochemical iodine-sulfur (IS) process, which uses nuclear heat to decompose water, is a potential method of hydrogen production without emitting carbon dioxide. The IS process consists of a coupling of three chemical reactions (Bunsen reaction, sulfuric acid decomposition, and hydrogen iodide decomposition). One challenge in the development of the IS process is the efficient separation of hydrogen from the other gases, hydrogen iodide and iodine, in the hydrogen iodide decomposition ($2\text{HI} \rightarrow \text{H}_2 + \text{I}_2$). No membrane has yet been developed that can efficiently separate H_2 while treating corrosive HI gas and high temperature. In this study, an industrial size (400 mm long) membrane with high separation performance and corrosion stability was developed by fabricating a three-layer structure consisting of a base α -alumina support tube, a middle silica layer and a top H_2 -selective silica layer. The middle and top silica layers were prepared by sol-gel dip-coating of tetraethoxysilane and chemical vapor deposition (CVD) of hexyltrimethoxysilane, respectively. By selecting the dipping time and CVD time, which are critical to the properties of the resulting silica layers, the prepared membrane showed high H_2/N_2 and H_2/SF_6 selectivities of 864 and 1672, and H_2 permeance of $2.4 \times 10^{-7} \text{ mol Pa}^{-1} \text{ m}^{-2} \text{ s}^{-1}$. HI stability tests also showed that the developed membrane was stable in corrosive HI environment. The H_2 -separation membranes developed in this study are suitable for membrane reactors that produce H_2 using HI decomposition in the thermochemical IS process.

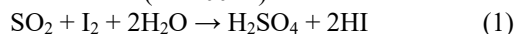
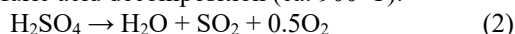
Keywords: hydrogen; nuclear energy; thermochemical cycle; hydrogen separation; ceramic membranes**Nomenclature**

IS	Iodine-sulfur
CVD	Chemical vapor deposition
HTMOS	Hexyltrimethoxysilane
TEOS	Tetraethoxysilane

1. Introduction

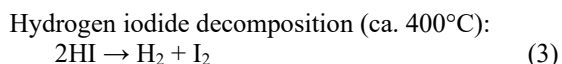
The Japanese government has set a goal of achieving carbon neutrality by 2050. To achieve this goal, carbon-free hydrogen production technology is essential. The thermochemical water-splitting iodine-sulfur (IS) process is considered as a promising carbon-free hydrogen production method, as it uses nuclear heat to decompose water to produce hydrogen. In this process, iodine (I_2) and sulfur dioxide (SO_2) are added to water, forming hydrogen

iodide (HI) and sulfuric acid (H_2SO_4) in an exothermic reaction. Under suitable conditions, these compounds are immiscible and can be easily separated. The H_2SO_4 can be decomposed at about 900°C , releasing the oxygen (O_2) and allowing the sulfur dioxide (SO_2) to be recycled. HI can be decomposed at about 400°C , releasing hydrogen (H_2) and allowing iodine (I_2) to be recycled. The chemical equations for this IS process are as follows:

Bunsen reaction (ca. 100°C):Sulfuric acid decomposition (ca. 900°C):

*Corresponding author.

E-mail: odtsetseg.myagmarjav@jaea.go.jp.



The net reaction is the decomposition of H_2O into H_2 and O_2 . The entire process requires only H_2O and high-temperature heat (900°C), releasing H_2 , O_2 , and low-temperature heat. This input temperature range is suitable for utilizing the nuclear heat supplied by high-temperature gas-cooled reactors. All reagents are recycled without routine effluent release.

The IS process was proposed by the General Atomics in 1976 [1] and has been widely studied worldwide during the past decades: the United States [2], France [3], South Korea [4], China [5], and Japan [6-8]. However, closed-cycle operation of the IS process has been done only rarely due to engineering and scientific difficulties. The Japan Atomic Energy Agency (JAEA) completed the first closed-cycle continuous operation at 1 NL h^{-1} in 1998, followed by a one-week demonstration of continuous H_2 production at 31 NL h^{-1} in a glass bench-scale facility in 2004, demonstrating the feasibility and controllability of the IS process [9]. In 2014, an integrated H_2 test facility made of industrial materials was constructed with H_2 production scale of 100 NL h^{-1} , as glass is not suitable for scale-up from a practical point of view. JAEA has successfully completed continuous H_2 production tests of 10 NL h^{-1} for 8 h in 2016 [6], 20 NL h^{-1} for 30 h in 2019 [8], and recently 30 NL h^{-1} for 150 h [10,11], which was a measure of stable operation.

Despite the continuous stable operation, improving the thermal efficiency of the IS process remains a challenge. One method to improve efficiency is the effective separation of H_2 from the other products, such as I_2 and HI, during HI decomposition, as its equilibrium conversion is only approximately 20% at 400°C . This means that nearly 80% of the HI feed has to be circulated, which is thermally inefficient and limits the practical application of the IS process. To increase the conversion rate of HI decomposition, it is necessary to use a membrane reactor equipped with H_2 separation membrane [12-16]. By extracting H_2 from the membrane reactor through the H_2 separation membrane, the reaction equilibrium is forced to shift based on Le Chatelier's principle, and more H_2 is produced. In the membrane reactor, the H_2 separation membrane plays a concrete measure.

HI decomposition occurs in a harsh environment with high temperatures ($>400^\circ\text{C}$) and corrosive HI gas, and thus common H_2 separation membranes such as polymeric membranes [17,18] and palladium membranes [19-21] are unsuitable. Therefore, the membrane materials that can be used for HI decomposition are mainly microporous ceramics, especially silica, due to their high thermal and chemical durability. The silica membranes are prepared by a sol-gel method [22-24] and chemical vapor deposition method (CVD) [25-28].

Silica membranes fabricated by sol-gel method generally provide high permeance but low selectivity. In contrast, the membranes fabricated by CVD method provide high H_2 selectivity but low permeance.

As H_2 purification during HI decomposition is a

emerging application of H_2 separation membrane, a few studies investigating the stability of silica membranes under corrosive HI gas have been reported in literature [29-31]. The first study on the corrosion stability of silica membrane was conducted by Hwang *et al.*, [29]. They prepared silica membranes by CVD method with a three-layer structure (base α -alumina support, middle γ -alumina layer, and top silica layer) and a two-layer structure without middle γ -alumina layer (base α -alumina support and top silica layer). The membrane without middle γ -alumina layer was more stable than membrane with middle γ -alumina layer for 150 h under HI- H_2O gaseous mixture. The same results were obtained by our group, where membranes with middle γ -alumina failed to demonstrate sufficient stability after 200 h in corrosive HI gas. On the other hand, the membranes with middle layer changed from γ -alumina to silica remained stable in corrosive HI gas for 300 h [31]. This result suggests that the Si-O-Si bond is stable during HI corrosion and can maintain its structure.

Despite their stability, scaling up the size of silica membrane is essential for practical applications and mass production. To date, the longest reported a three-layer structured membrane with a middle layer silica prepared by CVD measures 400 mm [31], whilst organo-silica membranes prepared by the sol-gel method has reached similar length [32]. The organo-silica membranes (diameter 12 mm ; length 400 mm) achieved H_2 permeance of $5.0 \times 10^{-7} \text{ mol Pa}^{-1} \text{ m}^{-2} \text{ s}^{-1}$, but their H_2/CH_4 selectivity was relatively low at 10.6. Additionally, the organo-silica membranes were open-ended, making them impractical for real-world applications. For technical viability, one end of the membrane tube must be closed to prevent thermal variations along its length, which can lead to mechanical instabilities and damage in the membranes, as well as to address sealing issues. In our previous work, we developed three-layer structured membrane with a middle silica layer prepared by CVD (diameter 10 mm ; length; 400 mm), with one-end closed, effectively mitigating thermal fluctuation and sealing challenges [31]. These three-layer structured membrane exhibited a high H_2/SF_6 selectivity of 1240 but had a moderate H_2 permeance of $1.4 \times 10^{-7} \text{ mol Pa}^{-1} \text{ m}^{-2} \text{ s}^{-1}$. However, further investigation into the reproducibility of membrane fabrication and its conditions, as well the impact of higher pressure on the H_2 production rate through membrane, is needed to discuss the potential of using this silica membrane in a membrane reactor for HI decomposition.

This study builds upon previous research by investigating the effects of fabrication conditions on membrane performance, particularly the dip-coating time for the middle silica layer formation and the deposition time for the top separation silica layer—both critical factors influencing membrane properties. The impact of pressure on the H_2 production rate, which is essential for the practical application of the developed membranes, was also investigated. Furthermore, the corrosion stability of the H_2 separation silica membrane was evaluated.

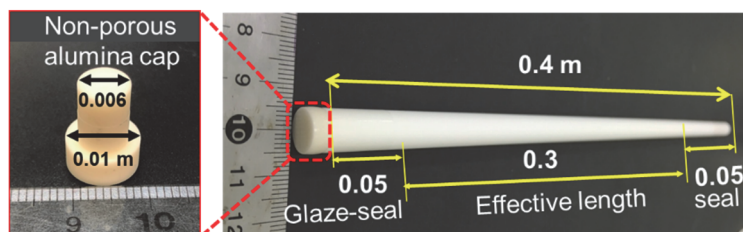


Figure 1. Image of a 400 mm dual-Si-layered membrane with one end closed.

2. Experimental

2.1. Membrane fabrication

The membranes were fabricated in a three-layer structure (a base α -alumina support, a middle silica layer and a top H_2 -selective silica layer). The membrane fabrication procedure and experimental setup are described elsewhere [31]. The membrane fabrication procedure is briefly described as follows. Cylindrical α -alumina porous supports with an inner diameter of 7 mm, an outer diameter of 10 mm, and a length of 400 mm were provided by Iwao Jiki Kogyo Co., Ltd. (Japan). It was symmetrical, with an average pore size of 125 nm and porosity of about 34%. To avoid damage to the membrane along its length due to thermal fluctuations and mechanical instability, one end of a 400 mm porous support tube was first closed with a nonporous alumina cap provided by Tokai-alumina Co., Ltd. (Japan). The tubes were glazed with SiO_2 -Ba-CaO sealant, except for a 300 mm effective length in the center.

Next, a middle silica layer was formed on the outer surface of support tube. This was prepared by dip coating method of silica sol. The silica sol was prepared by the sol-gel method, in which tetraethoxysilane (TEOS) was hydrolyzed with EtOH and HNO_3 in water (TEOS:EtOH: H_2O : HNO_3 = 1:5:4:0.1 mol%) to form colloidal silica sol by simultaneous condensation reaction. The mean diameter of the silica sol was measured to be approximately 9 nm using a nanoparticle analyzer (SZ-100, Horiba Co., Ltd). The end-closed support tubes were then immersed horizontally in the silica sol at a rate of 1 cm s^{-1} for 10, 30, and 60 s. Subsequently, the coated tubes were dried at 100°C for 1 h and calcined at 600°C for 3 h. The dipcoating, drying, and calcination processes were performed once. This silica-coated α -alumina support is called a Si substrate.

After preparing the Si substrate, an H_2 separation silica layer was formed as the top layer on the outer surface of the Si substrate by counter-diffusion CVD using hexyltrimethoxysilane (HTMOS) as the silica source. HTMOS was vaporized at 125°C with N_2 flow (200 mL min^{-1}) as carrier gas controlled by a mass flow controller and supplied to the outside of the membrane tube. Simultaneously, O_2 was supplied to the inside of the membrane tube at 20 mL min^{-1} . The module temperature was maintained at 450°C . The CVD time was varied between 20 and 120 min. The 400 mm long, silica-coated Si substrate with one end closed is referred to as a dual-Si-layered membrane (Figure 1).

2.2. Measurements of permeation performance and corrosion stability

The permeances of He (kinetic diameter = 0.26 nm), H_2 (0.29 nm), N_2 (0.36 nm), and SF_6 (0.55 nm), as single gases permeating through the membranes were measured in the temperature range of 26 – 450°C using a bubble flow meter and pressure difference methods. The measurements were conducted with the same apparatus used for the CVD experiments, which are described elsewhere [31]. The H_2 flux through the membrane was measured when the pressure was changed between 0.2 and 0.8 MPaG.

The stabilities of the dual-Si-layered membranes were examined by exposing them to corrosive HI gas and monitoring the N_2 permeance. The flow rate of the HI gas was maintained at 100 mL min^{-1} . The stability tests were performed at room temperature for about 20 h. After a certain time, the N_2 permeation test was conducted using bubble flow method as the stability indicator.

3. Results and Discussion

3.1. Evaluation of membrane performance

Figure 2 shows the permeances of H_2 , N_2 , and SF_6 measured at room temperature for the developed Si substrate (base α - Al_2O_3 support and middle silica layer) and dual-Si-layered membrane (base α - Al_2O_3 support, middle silica layer, and top silica layer). The results for bare α - Al_2O_3 support (without coating) were also included.

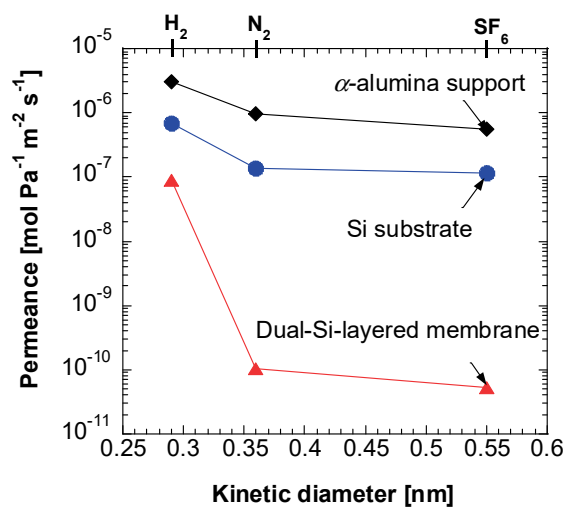


Figure 2. Comparisons of permeation performance of α - Al_2O_3 support (bare support), Si substrate, and dual-Si-layered membrane.

The permeances of all gases was in the order Support > Substrate > Membrane, indicating that the middle and top Si layers were successfully formed. Compared to the support and substrate, the membrane showed different trends, especially for N₂ and SF₆, where a significant decrease in permeances was observed due to the larger kinetic diameters of N₂ (0.36 nm) and SF₆ (0.55 nm). The difference in permeances leads to the selectivity, which is important for the purification of H₂ in membrane reactors. The developed membrane showed high selectivities of H₂/N₂ = 864 and H₂/SF₆ = 1672, which were much higher than the values recorded for the substrate (H₂/N₂ = 4.8 and H₂/SF₆ = 6.8). This result indicates that a top silica layer selective for H₂ was successfully formed on the substrate by CVD method without any defects and pinholes. From the selectivity results, it is assumed that the top silica layer has many small pores and a few large pores through which large gases pass. The recorded SF₆ permeance was as low as 5.2×10^{-11} mol Pa⁻¹ m⁻² s⁻¹, indicating no leakage occurred during the permeation tests.

Figure 3 shows the scanning electron microscopy (SEM; S-3000N, Hitachi Co., Ltd., Japan) micrographs of the surfaces (**a, b**) and cross sections (**c, d**) of the Si substrate and the dual-Si-layered membrane. In comparison with the substrate, there was no significant difference in the cross section of the membrane, but the surface was relatively smooth and importantly, no defects were observed. This result indicates that the counter-diffusion CVD process lets silica deposit inside the pores and uniformly form near the membrane surface because CVD has been widely used to deposit thin films on porous supports or drive chemically homogeneous deposition processes, especially those inside the pores of a support. This result is consistent with the results given in Figure 2, in which the permeances of gases, particularly, large gases of N₂ and SF₆ through the membrane were much smaller than that tested through the substrate, indicating that the top silica layer for H₂ separation was successfully formed on the surface of substrate.

Figure 4 compares permeation performances of the Si

substrate and the dual-Si-layered membrane as a function of the permeation temperature. As can be seen from Figure 4 (a), the permeance of each gas through the substrate decreased slightly with increasing permeation temperature. The corresponding selectivities were 4.8 - 8.4 for H₂/N₂ at 26-450°C and 5.8 - 6.1 for H₂/SF₆ at 26-200°C, respectively, which are close to the theoretical values for Knudsen diffusion, H₂/N₂ = 3.7 and H₂/SF₆ = 8.5. This small discrepancy is due to measurement error, but is negligible as the highly selective membranes were obtained after CVD procedure. This implies that our experimental technique is appropriate and reasonable. From the permeances recorded on the substrate, the gas permeation mechanism for the Si substrate is assumed to be Knudsen diffusion for all gases measured.

For the membrane (Figure 4 (b)), the permeances increased with increasing temperature, regardless of the gas. This suggests that activation diffusion is assumed to be dominant in the membrane. The membrane showed high selectivities of 30-864 for H₂/N₂ at 26-450°C and 1620-1672 for H₂/SF₆ at 26-200°C. The permeance of SF₆ was measured below 200°C to prevent membrane damage via its decomposition. These selectivities of the membrane were much higher than the substrate, suggesting that the top silica layer was well formed on the substrate and the top silica layer was selective to H₂. At 400°C, the target temperature of HI decomposition in the membrane reactor, the H₂ permeance of the developed membrane was 3.1×10^{-7} mol Pa⁻¹ m⁻² s⁻¹ and H₂/N₂ selectivity was 148. These values are close to the target values of 4.0×10^{-7} mol Pa⁻¹ m⁻² s⁻¹ (H₂ permeance) and 80 (H₂/N₂ selectivity) for the silica-based membrane reactor for HI decomposition [15,16], and thus the developed dual-Si-layered membrane in this study was considered to be a promising candidate.

3.2. Effects of membrane fabrication time

A characteristic that greatly affects the performance of H₂ separation membranes is the time required to form each silica layer of the dual-Si-layered membrane.

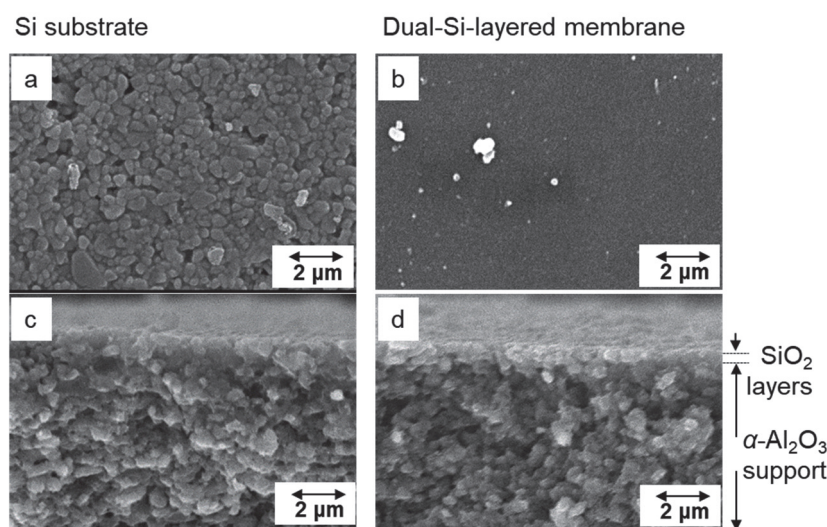


Figure 3. SEM micrographs of (a,b) the surface of, and (c,d) the cross-sections of a Si substrate and dual-Si-layered membrane.

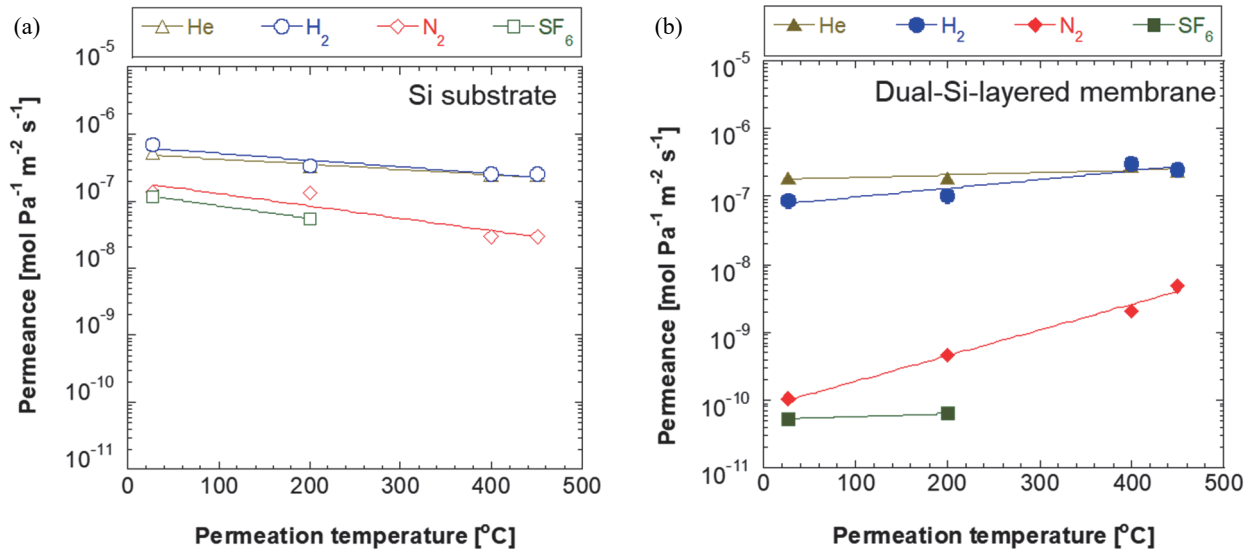


Figure 4. Temperature dependence of single-gas permeances through 400 mm long (a) Si substrate and (b) dual-Si-layered membrane with one end closed (CVD was carried out at 450°C for 20 min).

In this study, the dip-coating time to form the middle silica layer and the CVD time to form top separation silica layer were examined, respectively.

First, the effect of the dipping time on the permeation performance of the Si substrate was examined. **Figure 5** shows the H₂ permeances via substrate fabricated at three different dipping times (10, 30, and 60 s). The dipping time refers to the time (period) that the support tube was immersed in the silica sol. This figure also includes results for the α -alumina bare support and no coatings, which are indicated as 0 in the figure. The permeances for all gases were in the order of Support > Substrate 10 s > Substrate 30 s > Substrate 60 s. The α -alumina support exhibited highest permeances for all gases studied due to its large pore of 125 nm. By contrast, the substrates showed lower permeances than the α -alumina support due to its smaller pore size of about 3 nm, which was determined from the average diameter of the silica sol (about 9 nm). This result indicates that the middle silica layer was well formed on the α -alumina support. Furthermore, the permeances recorded on the substrate decreased with increasing dipping time. This was due to the deposition of more silica and the formation of a thicker layer.

The permeances of H₂ through the middle silica layer can be determined using a series analysis of gas diffusion, where the permeance through the silica layer only can be calculated by subtracting the resistance of support from the resistance of substrate:

$$\frac{1}{\bar{P}_{\text{Middle Si-layer}}} = \frac{1}{\bar{P}_{\text{Substrate}}} - \frac{1}{\bar{P}_{\text{Support}}} \quad (4)$$

where $\bar{P}_{\text{Middle Si-layer}}$ is the permeance through the middle silica layer, $\bar{P}_{\text{Substrate}}$ is the permeance through substrate, and \bar{P}_{Support} is the permeance through support. As the H₂ permeances through substrate and support are known, the permeance through the middle silica layer can be calculated. The H₂ permeances through the middle

silica layer only were calculated to be 7.7×10^{-7} , 2.7×10^{-7} , and 2.0×10^{-7} mol Pa⁻¹ m⁻² s⁻¹, for 10, 30, and 60 s respectively. In other words, there is no significant difference between the permeances of the substrate and middle silica layer only. This result indicates that the middle silica layer controls the permeance in the substrate, and the results for the middle silica layer are essentially the same as for the entire substrate.

As the reciprocal resistance is proportional to thickness, it was estimated that increasing the dipping time from 10 s to 30 s and 60 s would increase the thickness of the corresponding silica layer by a factor of approximately 2.9 and 3.8 respectively. In terms of permeation performance, a dipping time of 10 s is desirable to obtain higher H₂ production rates and this is taken into account in the following discussion.

Next, the effect of CVD time on the permeation performance of the dual-Si-layered membrane was

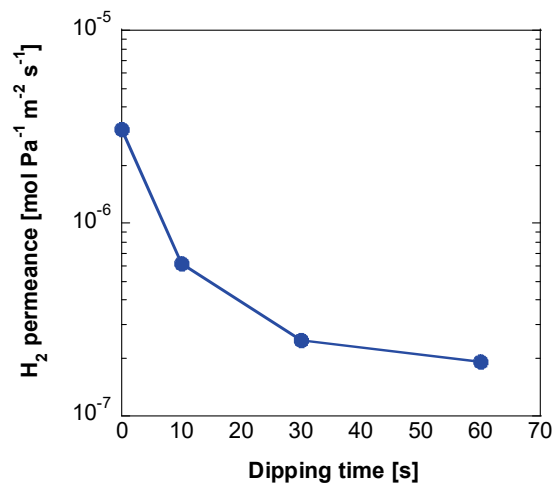


Figure 5. Effects of dipping time on H₂ permeances through the Si substrates.

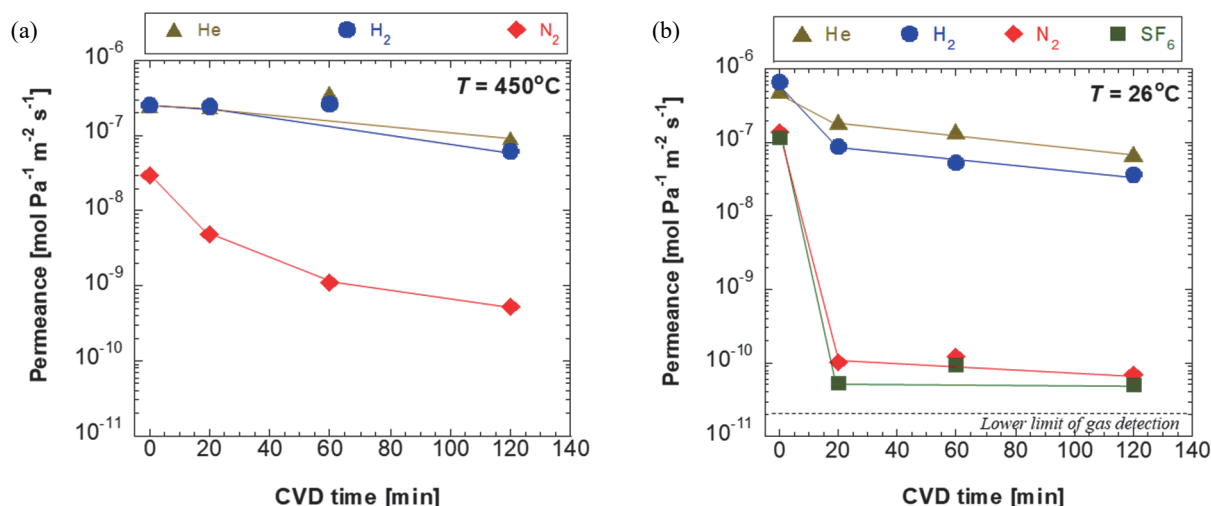


Figure 6. Effects of CVD time on He, H₂, and N₂ permeances through dual-Si-layered membrane at (a) 450°C and (b) room temperature.

investigated; the CVD time was varied between 20 and 120 min. The measurements were conducted at two different temperatures: high temperature (450°C) and low temperature (room temperature). **Figure 6 (a)** shows the results at the high temperature of 450°C. The permeances of the smaller gases, He and H₂ decreased slightly with CVD time, but remained above $1.0 \times 10^{-7} \text{ mol Pa}^{-1} \text{ m}^{-2} \text{ s}^{-1}$ even CVD time exceeded 60 min. On the other hand, the CVD time had a significant impact on the permeances, especially for the larger gas N₂; the H₂/N₂ selectivity increased from about 50 to 114 when the CVD time was extended from 20 to 120 min. Longer CVD time decreased the permeances but increased the selectivity. A similar trend was also observed for the permeances measured at low temperature of 26°C (**Figure 6 (b)**), with the permeances decreasing as the CVD time increased. Due to the detection limit of permeation test apparatus ($2.0 \times 10^{-11} \text{ mol Pa}^{-1} \text{ m}^{-2} \text{ s}^{-1}$), no significant difference in the permeances were observed, especially for N₂ and SF₆ when the CVD time was extended from 20 min to 120 min. However, the corresponded selectivities varied between 527 and 864 for H₂/N₂ and between 704 and 1672 for H₂/SF₆. The high selectivity suggests that more silica was deposited by CVD, creating small pores selective for H₂. In a similar way to that discussed in Figure 5, the permeances through only the top silica layer, formed by CVD, were calculated and did not differ significantly from the permeances through the entire membrane itself. This means that the top silica layer controls the permeance of the membrane. Furthermore, by extending the CVD time from 20 to 60 and 120 min, the thickness of the top silica layer was estimated to increase by approximately 4.9 and 10.5 times, respectively. As a result, the high selectivities of 864 and 1672 for H₂/N₂ and H₂/SF₆ and H₂ permeance of $2.4 \times 10^{-7} \text{ mol Pa}^{-1} \text{ m}^{-2} \text{ s}^{-1}$ were recorded for CVD time of 20 min. This performance was higher than that of one previously reported membrane with H₂/N₂ and H₂/SF₆ selectivities of 42 and 1240 and H₂ permeance of $1.4 \times 10^{-7} \text{ mol Pa}^{-1} \text{ m}^{-2} \text{ s}^{-1}$ [31]. A high selectivity and H₂ permeance suggest that 20 min is an appropriate CVD time for membrane fabrication in

membrane reactors due to the high H₂ permeance and selectivity requirements. Furthermore, membrane fabrication in this study also implies the reproducibility of 400 mm closed-end silica membrane supported on a silica-formed α -alumina tube fabricated by CVD.

3.3. Effects of pressure on H₂ production rate

From the viewpoint of practical application, a high H₂ production rate is required, which depends on operating pressure of the membrane reactor. Therefore, we investigated the effect of the pressure on H₂ production using the developed 400 mm long, one-ended closed dual-Si-layered membrane. The pressure was varied between 0.2 and 0.8 MPaG to obtain the high H₂ production rate. The measurement temperature was set at 400°C, the same as the target temperature for HI decomposition. The results are shown in **Figure 7**. The H₂ production showed a nearly linear trend with operating pressure, with the highest H₂ production at 0.8 MPaG. The overall fit was very good with regression coefficient of 0.99, indicating no sealing issues and no leakage. The developed dual-Si-

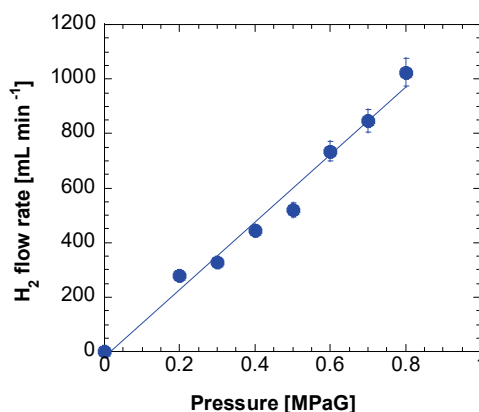


Figure 7. The relationship between pressure and H₂ flux measured through a 400 mm long dual-Si-layered membrane with one end closed.

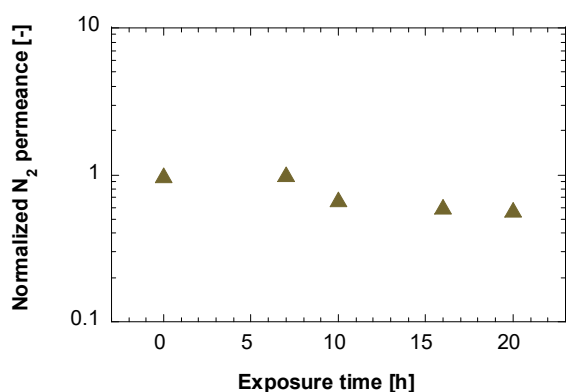


Figure 8. Stability of dual-Si-layered membrane under corrosive HI gas.

layered membrane was also confirmed to be stable under high pressure above 0.8 MPaG and high temperature of 400°C. In addition, based on these results, our technique for closing one end of membrane tubes was confirmed, which is important to avoid mechanical instability and membrane damage due to thermal fluctuations along the length of the membrane.

3.4. Evaluation of corrosion stability

Figure 8 shows the relationship between the HI exposure time and N₂ permeance through the dual-Si-layered membrane. The normalized N₂ permeance of 1 corresponds to N₂ permeance of $2.2 \times 10^{-9} \text{ mol Pa}^{-1} \text{ m}^{-2} \text{ s}^{-1}$, which measured before the HI corrosion tests. The N₂ permeance measured with the HI corrosion test apparatus was higher than that measured with the CVD apparatus. This is largely due to the difference in apparatus. That is, because of the highly corrosive HI gas, membrane fabrication and corrosion testing were performed on different equipment. Furthermore, it is possible that the membranes experienced complex temperature variations in a nitrogen atmosphere and humid air between the experiments; it has already been studied that a silica membrane prepared by CVD can be altered under such conditions. This may have led to the difference in permeances. Figure 8 shows that the dual-Si-layered membrane developed in this study was found to be stable in the presence of corrosive HI gas for over 20 h. For practical application, longer stability tests need to be considered and will be discussed in the next study. Thus, the dual-Si-layered membrane is expected to be applied to membrane reactors that decompose HI to produce H₂.

In summary, the dual-Si-layered membrane developed in this study is considered a promising candidate for a membrane reactor to decompose HI to produce H₂, as it showed high H₂ permeance, H₂/N₂ and H₂/SF₆ selectivities, corrosion stability and can be manufactured in an industrial shape with a length of 400 mm and is closed at one end to avoid thermal fluctuations along its length and sealing problems.

4. Conclusions

An H₂ separation membrane consisting of three layers (a base α -alumina support, a middle silica layer and a top

H₂-selective silica layer) was developed for application in a membrane reactor that decomposes HI to produce H₂. The effects of fabrication time on membrane performance, including dip-coating time for the middle silica layer formation and CVD time for the top separated silica layer, were investigated. These effects were significant, and the permeation performances increased with decreasing the fabrication time, with highest values recorded at 10 s of the dipping time and 20 min of CVD time. The dual-Si-layered membranes exhibited high H₂/SF₆ selectivity of 1672 and the H₂ permeance of $2.4 \times 10^{-7} \text{ mol Pa}^{-1} \text{ m}^{-2} \text{ s}^{-1}$. Furthermore, H₂ production showed a nearly linear trend with operating pressure, with the highest H₂ production at 0.8 MPaG. The developed membrane was also found to be stable even after exposure to corrosive HI gas for more than 20 h. In conclusion, the dual-Si-layered membrane developed in this study is considered a promising candidate for a membrane reactor to decompose HI to produce H₂ because it exhibited high permeance, selectivity, corrosion stability and can be fabricated in an industrial shape with a length of 400 mm and is closed at one end to avoid thermal fluctuations along its length and sealing problems.

References

- [1] J.L. Russell Jr., K.H. McCorkle, J.H. Norman, J.T. Porter II, T.S. Roemer, J.R. Schuster and R.S., Sharp, Water splitting - A progress report, in: 1st World Hydrogen Energy Conference (1976) pp. 1A105-1A124.
- [2] D. O'Keefe, C. Allen, G. Besenbruch, L. Brown, J. Norman, R. Sharp and K. McCorkle, Preliminary results from bench-scale testing of a sulfur-iodine thermochemical water-splitting cycle, *Int. J. Hydrogen Energy*. 7 (1982), pp. 381-392.
- [3] G. Cerri, C. Salvini, C. Corgnale, A. Giovannelli, D. De Lorenzo Manzano, A.O. Martinez, A. Le Duigou, J.M. Borgard and C. Mansilla, Sulfur-Iodine plant for large scale hydrogen production by nuclear power. *Int. J. Hydrogen Energy* 35 (2010), p4002-4014.
- [4] Y. Shin, T. Lee, K. Lee and M. Kim, Modeling and simulation of HI and H₂SO₄ thermal decomposers for a 50 NL/h sulfur-iodine hydrogen production test facility. *Appl. Energy*, 173 (2016), pp. 460-465.
- [5] P. Zhang, S.Z. Chen, L.J. Wang and J.M. Xu, Overview of nuclear hydrogen production research through iodine sulfur process at INET. *Int. J. Hydrogen Energy* 35 (2010), pp. 2883-2887.
- [6] N. Hiroki, K. Yu, T. Nobuyuki, T. Hiroaki, J. Iwatsuki, S. Kasahara, O. Myagmarjav and Y. Imai, ScienceDirect Hydrogen production using thermochemical water-splitting Iodine e Sulfur process test facility made, *Int. J. Hydrogen Energy*. (2020).
- [7] N. Sakaba, S. Kasahara, K. Onuki and K. Kunitomi, Conceptual design of hydrogen production system with thermochemical water-splitting iodine-sulphur process utilizing heat from the high-temperature gas-cooled reactor HTTR, *Int. J. Hydrogen Energy* 32 (2007), pp. 4160-4169.
- [8] H. Takegami, H. Noguchi, N. Tanaka, J. Iwatsuki, Y. Kamiji, S. Kasahara, Y. Imai, A. Terada and S. Kubo, Development of strength evaluation method of ceramic reactor for iodine-sulfur process and

- hydrogen production test in Japan Atomic Energy Agency, *Nucl. Eng. Des.* 360 (2020), p. 110498.
- [9] S. Kubo, H. Nakajima, S. Kasahara, S. Higashi, T. Masaki, H. Abe and K. Onuki, A demonstration study on a closed-cycle hydrogen production by the thermochemical water-splitting iodine - Sulfur process, in: *Nuclear Engineering and Design*, 233 (2004), pp. 347-354.
- [10] N. Hiroki, K. Yu, T. Nobuyuki, T. Hiroaki, I. Jin, K. Seiji, O. Myagmarjav, I. Yoshiyuki, K. Shinji, Hydrogen production using thermochemical water-splitting Iodine-Sulfur process test facility made of industrial structural materials: Engineering solutions to prevent iodine precipitation. *Int. J. Hydrogen Energy* 46 (2021), pp.22328-22343.
- [11] N. Tanaka, H. Takegami, H. Noguchi, Y. Kamiji, O. Myagmarjav and S. Kubo, Introduction of loop operating system to improve the stability of continuous hydrogen production for the thermochemical water-splitting iodine-sulfur process, *Int. J. Hydrogen Energy* 46 (2021), pp. 27891-27904.
- [12] N. Goswami, A., Bose, N. Das, S.N. Achary, A.K. Sahu, V. Karki, R.C. Bindal, S. Kar, DDR zeolite membrane reactor for enhanced HI decomposition in IS thermochemical process, *Int. J. Hydrogen Energy* 42 (2017), pp. 10867-10879.
- [13] O. Myagmarjav, N. Tanaka, M. Nomura, H. Noguchi, Y. Imai, Y. Kamiji, S. Kubo and H. Takegami, Development of a membrane reactor with a closed-end silica membrane for nuclear-heated hydrogen production. *Prog. Nucl. Energy* (2021), 103772.
- [14] O. Myagmarjav, N. Tanaka, M. Nomura and S. Kubo, Comparison of experimental and simulation results on catalytic HI decomposition in a silica-based ceramic membrane reactor, *Int. J. Hydrogen Energy* 44 (2019), pp. 30832-30839.
- [15] O. Myagmarjav, N. Tanaka, M. Nomura and S. Kubo, Hydrogen production tests by hydrogen iodide decomposition membrane reactor equipped with silica-based ceramics membrane, *Int. J. Hydrogen Energy* 42 (2017b), pp. 29091-29100.
- [16] M. Nomura, S. Easahara and S.I. Nakao, Silica membrane reactor for the thermochemical iodine-sulfur process to produce hydrogen. *Ind. Eng. Chem. Res.* 43 (2004).
- [17] M. Minelli, S. Oradei, M. Fiorini and G.C. Sarti, CO₂ plasticization effect on glassy polymeric membranes. *Polymer (Guildf)* 163 (2019), pp. 29-35.
- [18] L.M. Robeson, Correlation of separation factor versus permeability for polymeric membranes, *J. Memb. Sci.* 62 (1991), pp. 165-185.
- [19] M. Abdollahi, J. Yu, P.K.T. Liu, R. Ciora, M. Sahimi and T.T. Tsotsis, Ultra-pure hydrogen production from reformat mixtures using a palladium membrane reactor system. *J. Memb. Sci.* 390-391 (2012), pp. 32-42.
- [20] E. Fernandez, A. Helmi, J.A. Medrano, K. Coenen, A. Arratibel, J. Melendez, N.C.A. de Nooijer, V. Spallina, J.L. Viviente, J. Zuñiga, M. van Sint Annaland, D.A. Pacheco Tanaka and F. Gallucci, Palladium based membranes and membrane reactors for hydrogen production and purification: An overview of research activities at Tecnalia and TU/e. *Int. J. Hydrogen Energy.* 42 (2017), pp. 13763-13776.
- [21] D. Mendes, S. Sá, S. Tosti, J.M. Sousa, L.M. Madeira and A. Mendes, Experimental and modeling studies on the low-temperature water-gas shift reaction in a dense Pd-Ag packed-bed membrane reactor. *Chem. Eng. Sci.* 66 (2011), 2356-2367.
- [22] K. Kusakabe, S. Sakamoto, T. Saie and S. Morooka, Pore structure of silica membranes formed by a sol-gel technique using tetraethoxysilane and alkyltriethoxysilanes. *Sep. Purif. Technol.* 16 (1999), pp. 139-146.
- [23] H.F. Qureshi, A. Nijmeijer and L. Winnubst, Influence of sol-gel process parameters on the micro-structure and performance of hybrid silica membranes, *J. Memb. Sci.* 446 (2013), pp. 19-25.
- [24] K. Yoshida, Y. Hirano, H. Fujii, T. Tsuru and M. Asaeda, Hydrothermal stability and performance of silica-zirconia membranes for hydrogen separation in hydrothermal conditions, *J. Chem. Eng. Japan.* 34 (2001), pp. 523-530.
- [25] K. Akamatsu, M. Suzuki, A. Nakao and S. Nakao, *J. Memb. Sci.* 580 (2019), pp. 268-274.
- [26] S.J. Khatib and S.T. Oyama, Silica membranes for hydrogen separation prepared by chemical vapor deposition (CVD). *Sep. Purif. Technol.* 111 (2013). Pp. 20-42.
- [27] M. Nomura, T. Nagayo and K. Monma, Pore size control of a molecular sieve silica membrane prepared by a counter diffusion CVD method, *J. Chem. Eng. Japan* 40 (2007).
- [28] M. Nomura, K. Ono, S. Gopalakrishnan, T. Sugawara and S.I. Nakao, Preparation of a stable silica membrane by a counter diffusion chemical vapor deposition method, *J. Memb. Sci.* 251 (2005), pp. 151-158.
- [29] G.J. Hwang, J.W. Kim, H.S. Choi and K. Onuki, Stability of a silica membrane prepared by CVD using γ - and α -alumina tube as the support tube in the HI-H₂O gaseous mixture. *J. Memb. Sci.* 215 (2003), pp. 293-302.
- [30] O. Myagmarjav, A. Ikeda, N. Tanaka, S. Kubo and M. Nomura, Preparation of an H₂-permeable silica membrane for the separation of H₂ from the hydrogen iodide decomposition reaction in the iodine-sulfur process, *Int. J. Hydrogen Energy* 42 (2017a), pp. 6012-6023.
- [31] O. Myagmarjav, A. Shibata, N. Tanaka, H. Noguchi, S. Kubo, M. Nomura and H. Takegami, Fabrication, permeation, and corrosion stability measurements of silica membranes for HI decomposition in the thermochemical iodine-sulfur process. *Int. J. Hydrogen Energy* 46 (2021a), pp. 28435-28449.
- [32] K. Sawamura, S. Okamoto, Y. Todokoro, Development of mass production technology of highly permeable nano-porous supports for silicabased separation membranes. *Membranes* 9 (2019), pp.103-117.